Simulation of thermal drains using a new constitutive model for thermal volume change of normally consolidated clays

Radhavi A. Samarakoon, M.S.[1], and John S. McCartney, Ph.D., P.E., F.ASCE[2]

Abstract This paper focuses on the thermo-hydro-mechanical behavior of clay surrounding a thermal drain. A new constitutive model for prediction of thermal volume change of clays is presented that incorporates an improvement to existing models by capturing the effect of initial effective stress on the thermal volume change of normally consolidated clay observed in element-scale tests. A numerical framework with the proposed constitutive model was used to simulate the coupled effects of heat transfer, fluid flow and volume change in clay surrounding a thermal drain. The simulated results were validated using experimental data from a large-scale laboratory experiment on a thermal drain under different thermal and surcharge loads. The results indicate that the required surcharge can be reduced when using a thermal drain in lieu of a conventional vertical drain and a significant increase in the rate of consolidation is observed when using a thermal drain. The proposed constitutive model allows better prediction of thermal volume changes of normally consolidated clays as a function of depth which is important to understand the efficient application of in-situ heating for ground improvement.

Keywords: Thermal drain; Thermo-mechanical behavior; Constitutive model, Ground improvement; Soft clay

---

[1] Graduate Research Assistant, Department of Structural Engineering, University of California San Diego, La Jolla, CA 92093-0085, USA; Email: rabeysir@eng.ucsd.edu
[2] Professor and Department Chair, Department of Structural Engineering, University of California San Diego, La Jolla, CA 92093-0085, USA; Email: mccartney@ucsd.edu

1. Introduction

The use of thermal drains has been proposed as an approach to improve the mechanical properties of normally consolidated soft clays (Abuel-Naga et al. 2006; Pothiraksanon et al. 2010; Samarakoon and McCartney 2020a, 2021). A thermal drain combines a vertical drain used for radial consolidation of soft clay layers with a geothermal heat exchanger. The geothermal heat exchanger consists of a closed-loop, “U”-shaped pipe that transfers heat to the ground by circulating heated fluid through the pipe with a heat pump at the ground surface. The thermal drain itself can either be a prefabricated thermal drain consisting of a plastic strip with internal channels to support vertical water flow encased within a geotextile filter that is pushed into the clay, or a cylindrical borehole installed with a casing and backfilled with sand. The motivation for using thermal drains is twofold. First, the heating of the soft clay will lead to an increase in excess pore water pressure due to differential expansion of the pore water and soil solids (Mitchell and Campanella 1968; Ghabezloo and Sulem 2009; Ghaaowd et al. 2017). The thermal drain provides a drainage path for the pressurized water, and the consolidation process will result in contraction of the clay layer. Second, the increase in temperature will cause a reduction in water viscosity, which will result in an increase in hydraulic conductivity of the clay and an increase in the rate of consolidation (Houston et al. 1985). Thermal drains are best suited for normally consolidated and lightly overconsolidated clays, as heavily overconsolidated clays are expected to expand and contract elastically during heating and cooling, respectively (e.g., Baldi et al. 1988, Laloui and Cekerevac 2003; Abuel-Naga et al. 2007a, 2007b), although an increase in hydraulic conductivity would still be encountered in all clays. A typical deployment of thermal drains with a surface surcharge is shown in the schematic in Fig. 1.

An increase in the rate of consolidation as well as the magnitude of the ultimate surface settlement have been confirmed in calibration chamber experiments on thermal drains in soft clay layers that included comparisons with conventional drains (Abuel-Naga et al. 2006; Artidteang et al. 2011; Salager et al. 2012). The performance of thermal drains used in combination with a surficial surcharge load as part of the preconsolidation of a soft clay site was also investigated by Pothiraksanon et al. (2010). They applied a change in temperature of approximately 60 °C over the course of 200 days to a clay layer having a thickness of 8 m with a sand surcharge of 6 m, and observed a total settlement of approximately 400 mm for a thermal drain and 240 mm for a prefabricated vertical drain. An advantage of thermal drains over conventional vertical drains is that a surficial surcharge may not be necessary due to the thermal pressurization of the soft clay associated with heating of the drain. Bergenstahl et al. (1994) applied a change in temperature of approximately 60 °C to a 10 m-thick layer of clay over the course of 8.5 months using geothermal heat exchangers without vertical drains or the use of a surcharge and observed a thermally-induced settlement of 37 mm which was linked to the generation and dissipation of thermally-induced excess pore water pressures.

An issue that is critical to consider in the simulation of thermal drains in the field is the variation in expected thermal volume change as a function of depth in the clay layer. There is a growing set of data indicating that the thermal volume change in normally consolidated clays will change with its effective stress state (Samarakoon et al. 2018; Samarakoon and McCartney 2020b; Samarakoon et al. 2022). Furthermore, field-scale and laboratory studies (Bergenstahl et al. 1994; Abuel-Naga et al. 2007b; Uchaipichat and Khalili 2009; Ghaaowd et al. 2017) as well as poroelastic theories (Campanella and Mitchell 1968, Ghabezloo and Sulem 2009) show different thermal pressurization effects at different effectives stresses and void ratios during undrained heating of normally consolidated clays. The magnitude of thermal volumetric strains observed in the literature is relatively small, with an average of 1% volumetric strain occurring during a change in temperature of 60 °C. However, even a slight increase in thermo-plastic volumetric strain at a given depth will result in a significant improvement in clay mechanical properties as shown by Ghaaowd and McCartney (2021) and Ghaaowd et al. (2022) for pile pullout capacity and Samarakoon et al. (2022) for undrained shear strength of kaolinite specimens. Therefore, it is evident that the effect of effective stress state plays a critical role when simulating thermal drains in normally consolidated clays. To that end, the goal of this study is to develop a new constitutive model to predict the thermal volume change of normally consolidated clays which can be applied to studying the behavior of thermal drains. The model will be calibrated using data from thermal triaxial tests and used to simulate results from tank tests on thermal drains.

2. Background on Thermo-Mechanical Modeling of Saturated Clays

Several thermo-mechanical models have been developed by researchers to predict the thermal volume change of clay (Hueckel and Borsetto 1990; Cui et al. 2000; Laloui and Cekerevac 2003; Abeul-Naga et al. 2007a, Abuel-Naga et al. 2009). In general, the thermal volume change is dependent on the stress history. For overconsolidated clays, elastic expansion is expected upon heating with a tendency for contraction at higher temperatures, whereas for normally consolidated clays, plastic contraction can be observed. In some instances, lightly overconsolidated clays may also show contractive behavior (Baldi et al. 1988, Abuel-Naga et al. 2007b). Hueckel and Borsetto (1990) proposed a parabolic yield surface expression in the T-p' plane based on the evolution of preconsolidation stress with temperature which required the determination of multiple material parameters. At stress states below the yield limit, thermal strains will be elastic. If the yield limit is approached either by mechanical or thermal loading, plastic thermal strains will be generated, and the yield surface will move to the right due to thermal hardening resulting in a larger elastic zone.

Other studies have proposed different thermal yielding curves to capture trends observed in experimental data. For example, Cui et al. (2000) proposed a simplified relationship for the yield surface where an exponential expression was used as follows:

$$p_c{}'(T) = p_c{}'(T_0)\exp\left(-\alpha_0 \Delta T\right) \quad (1)$$

where $p_c'(T_0)$ is the apparent preconsolidation stress at room temperature, $p_c'(T)$ is the preconsolidation stress at temperature T, and α_0 is a material parameter. To better account for the effects of overconsolidation ratio (OCR) on volume change at high temperatures, Cui et al. (2000) introduced a second yield limit within the framework of Hueckel and Borsetto (1990). Specifically, the contractive behavior observed in overconsolidated clays at higher temperature was captured by this model.

An isotropic thermo-plastic yield limit was introduced by Laloui and Cekerevac (2003) with a logarithmic yield surface expression as follows:

$$p_c{}'(T) = p_c{}'(T_0)\left[1 - \gamma log\left(\frac{T}{T_0}\right)\right] \quad (2)$$

where γ is a material parameter. Abuel-Naga et al. (2007a) adopted the same relationship as that proposed by Laloui and Cekerevac (2003) in Eq. (2) for the loading yield limit, but used a similar approach to Cui et al. (2000) with two different yield limits referred to as the thermal and loading yield limit respectively.

An issue encountered in applying the different thermo-mechanical models listed above is that normally consolidated clays will all have the same thermal volume change regardless of the initial effective stress state, a finding that contradicts experimental studies on the thermal volume change of soft clays (Samarakoon et al. 2018, 2022) as well as the trends in thermally induced excess pore water pressures of normally consolidated soil with different initial effective stresses (Abuel-Naga et al. 2007b; Uchaipichat and Khalili 2009). The isotropic yield mechanism proposed by Laloui and Cekerevac (2003) is shown in Fig. 2 (a) in the T-p' plane along with a thermal loading path for a normally consolidated clay in red. When a normally consolidated clay (initially on the yield curve) is subjected to an increase in temperature from T_0 to T_1 at constant mean effective stress, the LY curve will shift to the right. As a result of this thermal hardening phenomenon, the clay will undergo a contractive thermo-plastic volumetric change. This is represented in the e-ln p' plane by a shift in the normally consolidated line to the left at temperature T_1 as shown in Fig. 2(b). Regardless of the initial mean effective stress of the normally consolidated clay, the same thermal volume change will be predicted by the model.

The reason for this shortcoming of available thermo-mechanical constitutive models in being able to capture the observed thermal volume change data from the literature perhaps lies in the approach by which the effect of temperature on the yield curve is defined, where the yield curve is defined by mechanically loading overconsolidated clays after heating to different temperatures and identifying the apparent preconsolidation stress (Eriksson 1989, Boudali et al. 1994, Sultan et al. 2002). These studies found that the slopes of the recompression curve before yielding as well as the compression curve after reaching normally consolidated conditions were independent of temperature. Only a few studies have characterized the thermal volume change of soft clays under multiple mean effective stresses (Abuel-Naga et al. 2007a; Samarakoon et al. 2018, 2022). Given that the volume change predictions for normally consolidated soils were made based on these observations, the existing models have an inherent issue in predicting the volume change for normally consolidated clays, which remains the same irrespective of the effective stress state (Fig. 2(b)).

3. Proposed framework for thermal volume change of normally consolidated clay

Based on the experimental evidence of thermal volume change of saturated normally consolidated clay in Samarakoon et al. (2022), a new thermo-elasto-plastic mechanism is required to accurately represent the thermal behavior of saturated clay at different initial mean effectives stresses. Volumetric strain can be generated due to mechanical and/or thermal loading. At stress states below the yield stress the strains will be elastic whereas plastic strains will be obtained at stress states at the yield limit. Based on the experimental observations, a new framework is proposed to obtain plastic volume changes under thermal loading at different initial isotropic stress states.

3.1. Thermo-elastic strains

Although the focus of this study was on the plastic volume changes of saturated normally consolidated clay subjected to thermal loading, the thermo-elastic relationships are presented for the completion of the proposed model. The thermo-elastic strain (ε_v^{Te}) generated by thermal loading is obtained by the following relationship:

$$d\varepsilon_v^{Te} = \alpha dT \quad (3)$$

where α is the drained volumetric thermal expansion coefficient of clay and T is the temperature. α can be determined using thermal volume change results of highly overconsolidated clays or from heating cooling cycles applied to normally consolidated clays with a slow cooling rate. Cui et al. (2000) considered α to be a constant parameter whereas other researchers defined the coefficient α as a function of temperature and the effective stress (Laloui 2001; Abuel-Naga et al. 2007a). The elastic strains generated due to mechanical loading are obtained as follows:

$$d\varepsilon_v^e = \frac{\kappa}{1+e_0}\frac{dp'}{p'} \qquad (4)$$

where κ is the slope of the recompression line, p' is the mean effective stress, and e_0 is the initial void ratio.

3.2. Thermo-plastic strains

When the stress state reaches a yield limit, thermo-plastic strains are developed. As described in section 1, the yield limit can be reached by mechanical loading or thermal loading at constant effective stress. The yield limit for isotropic conditions can be expressed as follows:

$$f = p' - p_c' = 0 \qquad (5)$$

where p_c' is the apparent preconsolidation stress. Several relationships are found in literature representing the thermal evolution of the preconsolidation stress (Hueckel and Borsetto 1990; Cui et al. 2000; Laloui and Cekerevac 2003). Based on experimental evidence, an extension to Eq. (2) is proposed where the parameter γ is a function of the mean preconsolidation stress $p_c'(T_0)$, as follows:

$$\gamma\left(p_c'(T_0)\right) = \frac{a}{p_c'(T_0)} + b \qquad (6)$$

where $p_c'(T_0)$ is the apparent preconsolidation stress at room temperature, which must be greater than zero, and a and b are constants depending on the material with $a < 0$ and $b > 0$, such that γ increases with increasing mean preconsolidation stress for normally consolidated clays. For $\gamma > 0$, the condition $p_c'(T_0) > -a/b$ must be satisfied. The reason for proposing that γ is a function of mean preconsolidation stress is that all overconsolidated soils corresponding to a given preconsolidation stress will have the same value of γ, which is consistent with the way that previous thermo-mechanical models were developed. The variation in apparent thermal preconsolidation stress with temperature at different initial mean effective stresses, having different γ values is shown in Fig. 3. Laloui & Cekerevac (2003) also reported different γ values for experimental data from Moritz (1995) for Swedish clay at different depths. Substituting Eq. (6) into Eq. (2) will yield the following relationship:

$$p_c{}'(T) = p_c{}'(T_0)\left[1 - b \times log\left(\frac{T}{T_0}\right)\right] - a \times log\left(\frac{T}{T_0}\right) \tag{7}$$

For a normally consolidated clay, its current stress state will be equal to the preconsolidation stress and hence will be on the yield limit. When the temperature is increased at constant effective stress, the clay will be subjected to thermal yielding to maintain the current stress state and a plastic thermal volume change will occur. Thermally induced plastic volumetric strain, ε_v^{Tp} is related to the change in preconsolidation stress with temperature, as follows:

$$d\varepsilon_v^{Tp} = \frac{\lambda - \kappa}{1+e_0} ln\left(\frac{p_c{}'(T_0)}{p_c{}'(T)}\right) \tag{8}$$

where $p_c'(T)$ is the preconsolidation stress at temperature T obtained from Eq. (7) and λ is the slope of the VCL. As the parameter γ changes with the preconsolidation stress, the thermal volume change at different mean effective stresses obtained from Eq. (8) will change for a normally consolidated clay. This is an improvement to the existing thermo-mechanical constitutive models where the same amount of thermal volume change is predicted for normally consolidated clays irrespective of their mean effective stress.

The proposed thermo-mechanical framework is shown in Fig. 4(a) and (b) respectively. Fig. 4(a) shows the thermal volume change in the *e* vs. ln *p'* plane. Path ABC shows the compression curve at room temperature T_0. Path DEF is obtained by increasing the temperature of normally consolidated clay from T_0 to T_1. $p_{c1}'(T_1)$ is the preconsolidation stress at temperature T_1. As a result of drained heating at $p_{c1}'(T_0)$, a thermo-plastic volume change of Δe_v^{Tp} will occur, which can be obtained using Eq. (8). If the clay was subjected to heating at a higher mean effective stress (i.e. $p_{c2}'(T_0)$), the yield stress will now move to point J along the NCL, and the corresponding apparent thermal preconsolidation stress will be at point H. At this stress state, a higher thermo-plastic volume change, denoted by the distance JK will be obtained. Paths DEF and HKI are both obtained at temperature T_1, where path DEF is associated with the apparent thermal preconsolidation stress corresponding to preconsolidation stress at room temperature, $p_{c1}'(T_0)$ *and path HKI* is associated with the apparent thermal preconsolidation stress corresponding to preconsolidation stress at room temperature, $p_{c2}'(T_0)$. In the existing thermo-mechanical models, the NCL shifts to the left as the temperature is increased. Based on the proposed model, the shift in the NCL is not only a function of temperature but also the mean effective stress for normally consolidated clays.

The corresponding thermo-mechanical paths in the T-p' plane are shown in Fig. 4(b). The specimen is subjected to mechanical loading from path A to B. From B to E, the specimen is heated under drained conditions where the temperature increases from T_0 to T_1. Curve BD shows the yield limit and the preconsolidation stress is reduced to $p_{c1}'(T_1)$ at temperature T_1. For heating at a higher mean effective stress, the path will follow ABJ for mechanical loading and JK for drained heating. The corresponding thermal preconsolidation stress will now be at point H following the curve JH. For normally consolidated clays subjected to drained heating, the yield curve will shift to the right due to thermal hardening. Once the specimen is cooled back to room temperature, the clay specimen will have a new preconsolidation stress which will be greater than the preconsolidation stress prior to heating. The yield limit after cooling is also shown in Fig. 4(b). This preconsolidation stress after a heating cooling cycle can be obtained from Eq. (7).

4. Model Calibration

To calibrate the proposed model, the experimental results from Samarakoon et al. (2022) are considered in this study. Samarakoon et al. (2022) conducted thermal triaxial tests on saturated normally consolidated kaolinite specimens at four different mean effective stresses. The specimens were first mechanically consolidated under isotropic conditions to a normally consolidated state and then subjected to drained heating where the temperature was increased to 60 °C. Finally, the specimens were sheared under undrained conditions at the elevated temperature. Normally consolidated specimens at mean effective stresses 230, 260, 290 and 320 kPa were considered. Contrary to the existing thermo-mechanical predictions, the thermal volume change obtained at each mean effective stress was different and showed an increasing trend as the mean effective stress increased. The new experimental evidence from tests conducted on normally consolidated clays reveals a limitation in the existing thermo-mechanical constitutive models when predicting thermal volume change in normally consolidated clays subjected to drained heating.

In addition to the slopes of the compression curve (κ and λ) for a given clay, the proposed model requires determination of variation in the parameter γ at different mean effective stresses through parameters *a* and *b*. At least two drained heating tests conducted on normally consolidated clay specimens at different initial mean effective stresses are required to obtain these parameters. Three tests may provide better accuracy when determining the required model parameters. Using the thermal volume change results at each mean effective stress for a given temperature, the thermal preconsolidation stress, $p_c'(T)$ corresponding to each mean effective stress can be obtained using Eq. (8). Using the $p_c'(T)$ values at each stress state, the γ parameter corresponding to each mean effective stress can be obtained using Eq. (2). Finally, Eq. (6) can be used to determine the parameters *a* and *b*. Alternatively, Eq. (7) can also be used to obtain the parameter *a* and *b* directly after determining $p_c'(T)$ values. The obtained γ values at each mean preconsolidation stress and the fitting of Eq. (6) to the experimental data of Samarakoon et al. (2022) are shown in Fig. 5 and the model parameters are summarized in Table 1. Back-predictions of the experimental data of Samarakoon et al. (2022) are shown in Fig. 6. In general, good agreement can be observed between the predictions and the experimental data and the increasing trend in thermal volumetric strain with increasing mean effective stress of normally consolidated clays is captured by the proposed model. The thermal volume change at the lower mean effective stresses is predicted well by the model whereas the thermal volume change at the higher mean effective stress value of 320 kPa is slightly underpredicted. The thermal volumetric strain value obtained at 290 kPa seems lower in comparison and could be due to experimental variability in the initial conditions of the sedimented clay specimens.

The established model can capture the effect of initial mean effective stress on the thermal volume change of normally consolidated clay where the thermal volumetric strain increases with increasing mean effective stress. This is an improvement to the existing thermo-mechanical constitutive models where the same amount of volume change is predicted for normally consolidated clay irrespective of its initial stress state. Further studies on multiple soil types considering a wider range of stress states will assist in strengthening the established relationships for soil parameters. Better predictions of thermal volume change in normally consolidated clays are important specifically in applications such as using in-situ heating for soil improvement. When the thermal volume changes at different mean effective stresses indicative of different depths can be accurately predicted, soil improvement can be strategically applied over different depths. This can also assist with designing efficient in-situ heating arrangements for soil improvement.

5. Application – Thermal Drain Analysis

The proposed constitutive model was applied in a numerical model developed to simulate a thermal vertical drain embedded in a soft clay layer inside a large-scale oedometer. The numerical model simulates the coupled phenomena of heat transfer, fluid flow and volume change in soft clay surrounding a thermal vertical drain. The theoretical framework, formulation of the numerical model, comparison with experimental results along with a parametric analysis on the performance of a thermal drain is described in the following sections.

5.1. Soil Domain Geometry

To simulate the behavior of a clay layer around a thermal drain, a finite soil domain representing a large-scale oedometer experiment by Artidteang et al. (2011) was considered in this study. The thermal drain is inserted at the center of a cylindrical specimen of height h and radius r and a surcharge is applied at the top of the specimen. A schematic diagram of the thermal drain arrangement in a finite soil domain is shown in Fig. 7. This geometry was selected as it was used to validate the numerical model using experimental results of Artidteang et al. (2011). Although this geometry does not represent the boundary conditions expected in a field deployment of thermal drains, it permits the effects of temperature and applied surcharge on the transient thermal consolidation process.

5.2. Theoretical Framework

5.2.1. Heat transfer

When a thermal drain is being used, the temperature of the surrounding soil will increase. Assuming that heat transfer through the soil medium will occur through conduction only, it can be modeled using Fourier's law and energy conservation principles. The thermal drain was considered as a line heat source where the vertical distribution of temperature was assumed to be uniform. The governing equation for conductive radial heat transfer through soil based on Fourier's law and conservation of energy will be simplified as follows in cylindrical coordinates.

$$\frac{\rho_s C}{\lambda_T}\frac{\partial T}{\partial t} = \frac{\partial^2 T}{\partial r^2} + \frac{1}{r}\frac{\partial T}{\partial r} \quad (9)$$

where ρ_s is the total density of soil, C is the specific heat capacity of the soil, λ_T is the thermal conductivity of the soil, and r is the radial distance. The thermal conductivity of the clay will be impacted by the volume changes occurring in the clay, where more heat conduction can occur through the soil particles as the void space reduces. The change in thermal conductivity with porosity was considered using a parallel model as follows (Dong et al. 2015):

$$\lambda_T = n\lambda_f + (1-n)\lambda_s \quad (10)$$

where n is the porosity, λ_f is the thermal conductivity of the pore water and λ_s is the thermal conductivity of the soil particles.

5.2.2. Fluid flow

An increase in temperature will impact the fluid flow through the porous media by thermally induced excess pore water pressures and increased hydraulic conductivity. Thermally induced excess pore water pressure is generated because of the differences in the coefficients of thermal expansion of soil particles and the pore fluid. The soil will undergo volumetric contraction as the excess pore water pressures are dissipated. Furthermore, an increase in temperature will decrease the density and viscosity of the pore fluid which will result in an increase in hydraulic conductivity. The relationship between hydraulic conductivity (k) with fluid and soil properties can be understood using the definition of the intrinsic permeability, K in Eq. (11):

$$K = \frac{k\eta_w}{\rho_w g} \tag{11}$$

where η_w is the dynamic viscosity of the fluid, ρ_w is the fluid density and g is the coefficient of gravity. Abuel-Naga et al. (2006) observed an increase in hydraulic conductivity with an increase in temperature for Bangkok clay. However, the intrinsic permeability was found to be independent of temperature. The density of water will vary with temperature according to the following relationship:

$$\frac{\partial \rho_w}{\partial t} = -\rho_w \alpha_w \frac{\partial T}{\partial t} \tag{12}$$

where α_w is the volumetric coefficient of thermal expansion of water. The fluid viscosity can be expressed as a function of temperature following the empirical relationship given by Hillel (1980) in Eq. (13).

$$\eta_w(T) = -0.00046575 \ln(T) + 0.00239138 \tag{13}$$

Fluid flow through the porous media can be expressed using principles of mass conservation. The governing equation in cylindrical coordinates will be reduced as shown for the geometry considered as follows:

$$\frac{\partial(\mathrm{n}\rho_\mathrm{w})}{\partial \mathrm{t}} = -\frac{1}{\mathrm{r}}\frac{\partial(\mathrm{r}\rho_\mathrm{w}\mathrm{v})}{\partial \mathrm{r}} \tag{14}$$

where *v* is the fluid velocity. Fluid velocity for a porous medium can be expressed using Darcy's law as follows:

$$\mathrm{v} = -\frac{\mathrm{K}}{\eta_\mathrm{w}}\frac{\partial \mathrm{U}}{\partial \mathrm{r}} \quad (15)$$

where *U* is the pore water pressure. By substituting Eq. (15) into Eq. (14) and using the product rule, the following equation is obtained:

$$\mathrm{n}\frac{\partial \rho_\mathrm{w}}{\partial \mathrm{t}} + \rho_\mathrm{w}\frac{\partial \mathrm{n}}{\partial \mathrm{t}} = \frac{\mathrm{K}}{\eta_\mathrm{w}}\left(\rho_\mathrm{w}\frac{\partial^2 \mathrm{U}}{\partial \mathrm{r}^2} + \frac{\rho_\mathrm{w}}{\mathrm{r}}\frac{\partial \mathrm{U}}{\partial \mathrm{r}} + \frac{\partial \mathrm{U}}{\partial \mathrm{r}}\frac{\partial \rho_\mathrm{w}}{\partial \mathrm{r}}\right) \quad (16)$$

The effects of temperature on density and viscosity can be incorporated by substituting Eqs. (12) and (13) into Eq. (16). Considering the spatial variation of fluid density to be negligible, a general equation for non-isothermal fluid flow through porous media is obtained as follows:

$$-\mathrm{n}\alpha_\mathrm{w}\frac{\partial \mathrm{T}}{\partial \mathrm{t}} + \frac{\partial \mathrm{n}}{\partial \mathrm{t}} = \frac{\mathrm{K}}{\eta_\mathrm{w}}\left(\frac{\partial^2 \mathrm{U}}{\partial \mathrm{r}^2} + \frac{1}{\mathrm{r}}\frac{\partial \mathrm{U}}{\partial \mathrm{r}}\right) \quad (17)$$

5.2.3. Volume Change

The volume change in a thermal drain application will consist of mechanical and thermal components. The mechanical volume change due to application of a surficial surcharge can be obtained using compressibility relationships for a normally consolidated clay, given as follows:

$$\partial e^p = \lambda\frac{\partial p_v'}{p_v'} \quad (18)$$

where p_v' is the vertical effective stress. The thermo-plastic volume changes are obtained using the proposed constitutive relationship using Eqs. (7) and (8). For a simultaneous application of a surcharge and heat, the total stress will remain constant. The change in effective stress resulting from a change in the pore water pressure can be obtained by subtracting the pore water pressure from the total stress, *p* as follows:

$$p' = p - U \quad (19)$$

For lightly overconsolidated clays, the thermal volume change will consist of elastic as well as plastic components. For stress states below the yield limit, thermo-elastic strains will be generated as obtained by Eq. (3). As the temperature increases and the preconsolidation stress decreases, the soil will be subjected to thermal yielding and thermo-plastic strains will be generated (Eqs. (7) and (8)). The scope of the current study is limited to the simulation of thermal volume change of normally consolidated clays. However, the simulation can be extended to lightly overconsolidated clays by identifying the stress, temperature combination at the yield limit and obtaining the corresponding elastic and plastic components of the thermal volume change.

5.3. Boundary and Initial Conditions

The boundary conditions evaluated in this study are representative of a large-scale oedometer which was used for the validation of the numerical model. Heat transfer and fluid flow were considered to be axisymmetric about the axis of the drain for the numerical simulation. The variation of temperature in the vertical direction was assumed to be uniform thereby simplifying the geometry to a radial drainage problem. The thermal drain is treated as a line heat source where an elevated temperature will be applied. A constant temperature boundary condition was imposed at the thermal drain whereas a convective temperature boundary condition was maintained at the outer edges of the clay layer to represent the edges of a container in the laboratory. This outer boundary can be represented based on the experimental setup. For example, a constant temperature boundary condition or a function accounting for daily temperature fluctuations can be used when the outer boundary is maintained at ambient temperature. On the other hand, a convective boundary condition can be used to account for heat loss or zero heat flux to model thermal insulation at the boundary. A similar approach can also be used to model the surface temperatures.

Although not required, thermal drains are typically combined with an application of a surcharge on top of the saturated clay layer. The clay layer was assumed to be normally consolidated under the surcharge stress. The outer edge of the oedometer permits zero radial strain. However, a variation in void ratio within the clay layer with radius is expected due to heating from the central thermal drain. The surcharge is applied in stress-control conditions so settlements in the clay layer can be nonuniform as a function of the radius from the thermal drain. Drainage was only permitted at the location of the thermal drain (i.e., no vertical drainage from the top and bottom of the cylinder or radial drainage from the outer boundary). Accordingly, a constant hydrostatic pressure boundary was also applied at the drain location and the fluid velocity at the outer edge of the clay layer was taken as zero (i.e., no flow) representative of a large-scale oedometer. In a field application where multiple drains are used, the influence of other drains in the vicinity will have to be considered. For instance, multiple drain locations will be at constant temperature and hydrostatic pressure boundary conditions. Although not within the scope of this study, a more complex analysis with multiple drains will aid in determining the optimum spacing arrangements for thermal drains. The initial temperature in the soil domain was taken as equal to ambient temperature and the initial pore water pressure was determined based on the hydrostatic conditions and the applied surcharge. The initial porosity was determined based on the clay.

5.4. Numerical Formulation

The coupled phenomena were simulated using the finite difference method. Both steady state as well as transient variations in temperature, pore water pressure and settlement were solved for using the numerical model. The soil layer along a radius was spatially discretized into elements of equal size. A central difference scheme was used in the spatial domain and a forward difference scheme was used in the time domain. The numerical formulation was implemented and solved using Matlab.

5.5. Comparison with Experimental Data

The thermo-hydro-mechanical behavior of a saturated normally consolidated clay layer surrounding a thermal drain was simulated using the numerical model and compared with experimental data from literature. Artidteang et al. (2011) investigated the performance of a single thermal drain in soft Bangkok clay using a large-scale oedometer similar to the arrangement shown in Fig. 7. The clay layer was of diameter of 0.45 m and height of 0.7 m. The tests conducted using a conventional drain and a thermal drain were considered for the comparison in this study. In both tests, the clay specimens were first allowed to reach 90% consolidation under a surcharge of 50 kPa. For the specimen with a conventional drain, an additional surcharge of 50 kPa was applied whereas for the specimen with a thermal drain, a 50 kPa surcharge and heat up to 90 °C was applied simultaneously. To simulate this setup, an axisymmetric domain with a length of 0.225 m was considered and divided into elements of size 0.0225 m. A constant temperature of 90 °C was applied at the thermal drain and a convective boundary was imposed at the outer edge of the oedometer. The initial temperature was taken as 25 °C and the initial porosity was assumed to be 0.6. The hydrostatic pressures were determined considering a mid-depth of the soil specimen.

Based on the trends observed in experimental data of Samarakoon et al. (2022) and data from Abuel-Naga et al. (2007a) a relationship for the change in parameter γ with the mean preconsolidation stress was obtained as shown in Fig. 8. The material parameters for Bangkok clay used in the numerical model were estimated based on data from Artidteang et al. (2011) and Abuel-Naga et al. (2007a) and are summarized in Table 2. The predicted time series of temperature along with the corresponding data from Artidteang et al. (2011) are shown in Fig. 9. Close agreement is observed between the experimental results and the numerical simulation, specifically at locations further away from the thermal drain (Root-mean-square deviation (RMSD) = 2.65 for r = 200 mm). The temperature is slightly underestimated at locations closer to the drain (RMSD = 9.99 for r = 25 mm). Convective heat transfer not being considered and the assumed values of certain material properties may have resulted in the differences observed. Fig. 10 shows the comparison between simulated results for settlement of the clay specimen and the experimental data. The settlements obtained for the tests conducted with the conventional drain at room temperature as well as with a thermal drain with heating up to 90 °C are presented and were obtained at a radial distance of 112.5 mm. The simulated results closely match the experimental data where the increase in both the rate and magnitude of settlement obtained from a thermal drain is captured(RMSD = 16.1 for conventional drain and RMSD = 18.1 for thermal drain). The experimental data and the predicted results for the excess pore water pressure generated when using a thermal drain is shown in Fig. 11. Although a difference in the magnitude of the maximum excess pore water pressure is observed, the numerical model captures the trend in dissipation of excess pore water pressure well (RMSD = 24.4).

One reason for the differences in the predicted results and the data for settlement when using a thermal drain is the possible errors in estimating parameter γ. The relationship in Fig. 8 is based on limited data and has a low coefficient of determination (R^2). This can be improved by including additional data points for Bangkok clay obtained by conducting drained heating tests on normally consolidated specimens at different mean effective stresses. A change in γ will impact thermo-plastic strains where a higher γ value will result in a higher settlement. For instance, in this oedometer test predictions, a $\pm$10% change in γ will result in a $\pm$1.6% change in the maximum settlement obtained. Abuel-Naga et al. (2007a) reported a value of 0.43 for γ and the proposed relationship in this study allows γ to vary between 0.44-0.45 for the stress range considered. Although the proposed model adequately captures the thermal behavior of normally consolidated clay, better estimates of material properties will help further improve the accuracy of predicted results.

5.6. Parametric Analysis of Thermal Drain Performance in Normally Consolidated Clay

The validated numerical model was used to simulate the clay behavior surrounding a thermal drain, considering different variables of interest. Specifically, the impact on consolidation settlement due to the magnitude of applied temperature and surcharge load was investigated. A set up similar to that of Artidteang et al. (2011) with a Bangkok clay specimen of 0.7 m height and 0.45 m diameter was considered in the numerical simulation. Consolidation settlements obtained with a thermal drain operating at different temperatures under a surcharge of 100 kPa are shown in Fig. 12. An increase in the magnitude as well as the rate of settlement is observed as the temperature of the thermal drain is increased, conforming with the observations made in literature. Fig. 13 shows a comparison of the settlements obtained when using a conventional drain and a thermal drain operated at 90 °C, combined with a surcharge of 10, 25, 50 and 100 kPa respectively. An increase in the magnitude of settlement can be observed when using a thermal drain which will allow the required amount of surcharge to achieve a desired level of consolidation to be reduced. For instance, almost the same amount of consolidation settlement obtained using a conventional drain with 25 kPa surcharge can be obtained with a thermal drain operating at 90 °C combined with only 10 kPa surcharge.

The maximum settlement obtained at each surcharge value is summarized in Fig. 14(a). As it can be seen from the figure, the contribution of thermal volume change on the total settlement is more significant at lower surcharge values. The increase in the maximum settlement obtained when using a thermal drain is shown in Fig. 14(b). This increase can be attributed to the thermo-mechanical volume changes in the clay as a result of increasing the temperature. As described by the proposed constitutive model, the thermo-mechanical volume change can be observed to increase as the surcharge increases for normally consolidated Bangkok clay. The relationship obtained for Bangkok clay shows a small increase in parameter γ with the mean preconsolidation stress. As a result, the increase observed in thermo-mechanical volume change with surcharge is not significant. On the other hand, this increase may be more pronounced for other clay types such as kaolinite where the rate of increase in parameter γ with mean preconsolidation stress is more considerable.

The settlement obtained at different depths was also investigated using the numerical model simulating a large oedometer setup. A comparison of settlements obtained when using a thermal drain operating at 90 °C and a conventional drain under a surcharge of 25 kPa are shown in Fig. 15. Consolidation settlement at depths 0.15, 0.25 and 0.35 m were considered. Similar to the previous observations, an increase in the magnitude as well as the rate of settlement is observed when a thermal drain is used. Furthermore, the increase in the magnitude of settlement can be seen to increase with depth. Based on the above analysis, the surcharge required during preconsolidation can be reduced when using a thermal drain. In addition, there are significant savings with respect to time for consolidation. An optimum combination of temperature and surcharge can be determined based on factors such as soil geometry, soil properties and initial conditions, structural load, financial and time constraints. As the thermal improvement of the clay can also be expected to depend on the depth, the temperature increments can be strategically targeted with depth. Specifically, greater temperatures can be applied closer to the surface to lead to a uniform change in volume with depth using a thermal drain. This may occur naturally due to the dissipation of heat along the length of a geothermal heat exchanger (McCartney and Murphy 2017). The numerical analysis in this study was conducted using a single thermal drain. In a field application, however, the use of multiple thermal drains will have to be considered. Although not within the scope of this study, this analysis can be extended to investigate the performance of multiple thermal drains by considering the intersection of thermal and hydraulic influence zones surrounding each thermal drain. Furthermore, future studies on the cost savings associated with using the thermal drains after ground improvement to provide heat exchange or heat storage may help further justify the use of this technology. The stress-dependent observations in this study apply to normally consolidated clays but may also apply to lightly overconsolidated clays, which are even more widely encountered in nature than normally consolidated clays. Further research on the thermo-mechanical behavior of lightly overconsolidated clays is needed.

6. Conclusion

A new constitutive thermo-mechanical framework for predicting thermal volume change of soft clays is presented in this study. The proposed model can capture the increase in thermal volume change with increasing mean effective stress observed in experimental studies for normally consolidated clays. The model was applied in a numerical simulation of a thermal drain embedded in a soft clay deposit where coupled interactions of heat flow, fluid flow and volume change were considered. The simulated results were validated with experimental data available in literature. A parametric analysis conducted considering the effects of temperature and the surcharge applied shows that the use of a thermal drain has the potential to reduce the required amount of surcharge and significantly increase the rate of consolidation in comparison to a conventional vertical drain. The results demonstrate that the use of thermal drains can be a promising method of ground improvement while also having the potential to be used as heat exchangers subsequently, permitting sustainable and cost-effective energy usage for the building. Further analysis can be carried out considering different clay types and to determine optimal drain arrangements in field applications.

Acknowledgements

Funding from NSF grant CMMI 1941571 is appreciated. The opinions are those of the authors.

References

Abuel-Naga, H.M., Bergado, D.T., Chaiprakaikeow, S. (2006). "Innovative thermal technique for enhancing the performance of prefabricated vertical drain during the preloading process." *Geotextiles and Geomembranes*. 24, 359-370.

Abuel-Naga, H.M., Bergado, D.T., Bouazza, A., Ramana, G.V. (2007a). "Volume change behaviour of saturated clays under drained heating conditions: experimental results and constitutive modeling." *Canadian Geotechnical Journal*. 44, 942-956.

Abuel-Naga, H.M., Bergado, D.T., Bouazza, A. (2007b). "Thermally induced volume change and excess pore water pressure of soft Bangkok clay." *Engineering Geology*. 89, 144-154.

Abuel-Naga, H.M., Bergado, D.T., Bouazza, A., Pender, M. (2009). "Thermomechanical model for saturated clays." *Géotechnique*. 59(3), 273-278.

Artidteang, S., Bergado, D.T., Saowapakpiboon, J., Teerachaikulpanich, N., Kumar, A. (2011). "Enhancement of efficiency of prefabricated vertical drains using surcharge, vacuum and heat preloading." *Geosynthetics International.* 18(1), 35-47.

Baldi, G., Hueckel, T., Pellegrini, R. (1988). "Thermal volume changes of the mineral-water system in low-porosity clay soils." *Canadian Geotechnical Journal*. 25, 807-825.

Bergenstahl, L., Gabrielsson, A., Mulabdic, M. (1994). "Changes in soft clay caused by increase in temperature." *Proceedings of the 13th International Conference on Soil Mechanics and Foundation Engineering*. New Delhi, India. Jan 5-10. 1637-1641.

Boudali, M., Leroueil, S., Srinivasa Murthy, B.R. (1994). "Viscous behaviour of natural clays." *Proceedings of the 13th International Conference on Soil Mechanics and Foundation Engineering*. New Delhi, India. Jan 5-10. 411-416.

Brandl, H. (2006). “Energy foundations and other thermo-active ground structures.” *Géotechnique*. 56(2), 81-122.

Campanella, R.G., Mitchell, J.K. (1968). “Influence of temperature variations on soil behavior.” *Journal of the Soil Mechanics and Foundation Division. ASCE*. 94(3), 709-734.

Cui, Y. J., Sultan, N., Delage, P. (2000). “A thermomechanical model for clays.” *Canadian Geotechnical Journal.* 37(3), 607–620.

Dong, Y., McCartney, J.S., Lu, N. (2015). “Critical review of thermal conductivity models for unsaturated soils.” *Geotechnical and Geological Engineering.* 33, 207-221.

Eriksson, L.G. (1989). “Temperature effects on consolidation properties of sulphide clays.” *12th International Conference on Soil Mechanics and Foundation Engineering.* Rio de Janeiro. 2087-2090.

Gens, A., Olivella, S. (2001). “Clay barriers in radioactive waste disposal.” *Revue Française de Génie Civil*. 5(6), 845-856.

Ghaaowd, I., Takai, A., Katsumi, T., McCarntey, J.S. (2017). “Pore water pressure prediction for undrained heating of soils.” *Environmental Geotechnics*. 4(2), 70-78.

Ghaaowd, I., McCartney, J.S. (2021). “Centrifuge modeling methodology for energy pile pullout from saturated soft clay.” *ASTM Geotechnical Testing Journal*. 45(2), 332-354.

Ghaaowd, I., McCartney, J.S., Saboya, Jr., F. (2022). “Centrifuge modeling of temperature effects on the pullout capacity of torpedo piles in soft clay.” *Soils and Rocks. Special Issue on Energy Piles*. 45(1), e2022000822.

Ghabezloo, S., Sulem, J. (2009). “Stress dependent thermal pressurization of a fluid-saturated rock.” *Rock Mechanics and Rock Engineering*. 42(1), 1-24.

Hillel, D. (1980). *Fundamentals of Soil Physics.* Academic Press. New York, NY, USA.

Houston, S.L., Houston, W.N., Williams, N.D. (1985). "Thermo-mechanical behavior of seafloor sediments." *Journal of Geotechnical Engineering*. 111(12), 1249-1263.

Hueckel, T., Borsetto, M. (1990). "Thermoplasticity of saturated soils and shales: constitutive equations." *Journal of Geotechnical Engineering*. 116(12), 1765–1777.

Hueckel, T., Pellegrini, R. (1992). "Effective stress and water pressure in saturated clays during heating-cooling cycles." *Canadian Geotechnical Journal* 29, 1095-1102.

Laloui, L. (2001). "Thermo-mechanical behaviour of soils." *Revue Française de Génie Civil*. 5(6), 809-843.

Laloui, L., Cekerevac, C. (2003). "Thermo-plasticity of clays: an isotropic yield mechanism." *Computers and Geotechnics*. 30(8), 649–660.

McCartney, J.S. and Murphy, K.D. (2017). "Investigation of potential dragdown/uplift effects on energy piles." Geomechanics for Energy and the Environment. 10(June), 21-28. DOI: 10.1016/j.gete.2017.03.001.

Moritz, L. (1995). "Geotechnical properties of clay at elevated temperatures." *Report No 47 Swedish Geotechnical Institute*.

Pothiraksanon, C., Bergado, D.T., Abuel-Naga, H.M. (2010). "Full-scale embankment consolidation test using prefabricated vertical thermal drains." *Soils and Foundations*. 50(5), 599-608.

Salager, S., Laloui, L. and Nuth, M. (2012). "Efficiency of thermal vertical drains for the consolidation of soils." *2nd International Conference on Transportation Geotechnics*. Hokaido, Japan. 1-10.

Samarakoon, R.A., Ghaaowd, I., McCartney, J. S. (2018). “Impact of drained heating and cooling on undrained shear strength of normally consolidated clay.” *Proceedings of the 2nd International Symposium on Energy Geotechnics*. Lausanne, Switzerland. Sep. 26-28. A. Ferrari, L. Laloui, eds., Vienna. 243-249.

Samarakoon, R.A., McCartney, J.S. (2020a). “Analysis of thermal drains in soft clay.” *GeoAmericas 2020: 4th PanAm Conference on Geosynthetics*. Rio de Janeiro, Brazil. Oct 26-31. 1-9.

Samarakoon, R.A., McCartney, J.S. (2020b). “Role of initial effective stress on the thermal consolidation of normally consolidated clays.” *Proceedings of the 2nd International Conference on Energy Geotechnics (ICEGT-2020)*. E3S Web of Conferences, Les Ulis, France. 205, 09001. https://doi.org/10.1051/e3sconf/202020509001.

Samarakoon, R.A., McCartney, J.S. (2021). “Performance of prefabricated thermal drains in soft clay.” *Geosynthetics Conference 2021*. Kansas City, MO, USA. Feb 21-24. Nicks, J. and Beauregard, M., eds. IFAI, Roseville, MI. 1-12.

Samarakoon, R.A., Kreitzer, I.L., McCartney, J.S. (2022). “Impact of initial effective stress on the thermo-mechanical behavior of normally consolidated clay.” *Geomechanics for Energy and the Environment* [In Review].

Sultan, N., Delage, P., Cui, Y.J. (2002). “Temperature effects on the volume change behaviour of Boom clay.” *Engineering Geology.* 64, 135-145.

Uchaipichat, A., Khalili, N. (2009). “Experimental investigation of thermo-hydro-mechanical behaviour of an unsaturated silt.” *Géotechnique*. 59(4), 339–353.

Table 1 Model parameters for Georgia kaolinite clay

Parameter	Value
Slope of VCL (λ)	0.09
Slope of RCL (κ)	0.02
a	-238.7
b	1.2563

Table 2 Material parameters for Bangkok clay (Artidteang et al. 2011; Abuel-Naga et al. 2007)

Parameter	Value
Total unit weight (kN/m^3)	14.7
Initial porosity	0.6
λ (slope of VCL)	0.59
κ (slope of RCL)	0.1
γ (soil parameter)	$-0.69p_c'(T_0) + 0.46$
Thermal conductivity of soil particles (W/m/°C)	1.9
Thermal conductivity of pore water (W/m/°C)	0.6
Specific heat capacity (J/kg/°C)	1500
Intrinsic permeability (m^2)	1.0×10^{-16}

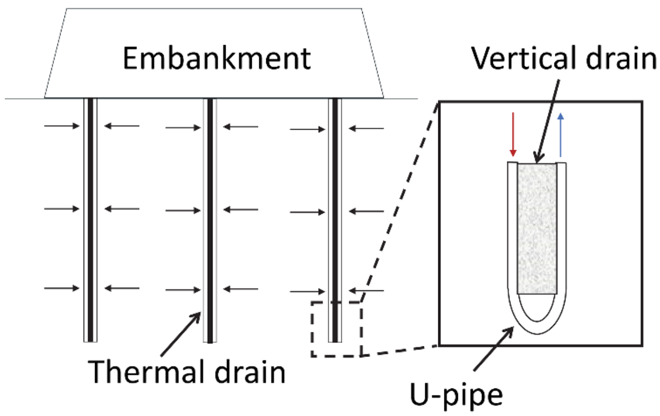

Fig. 1. Schematic of thermal drains embedded in a soil layer with a detail showing fluid flow in a closed-loop heat exchanger

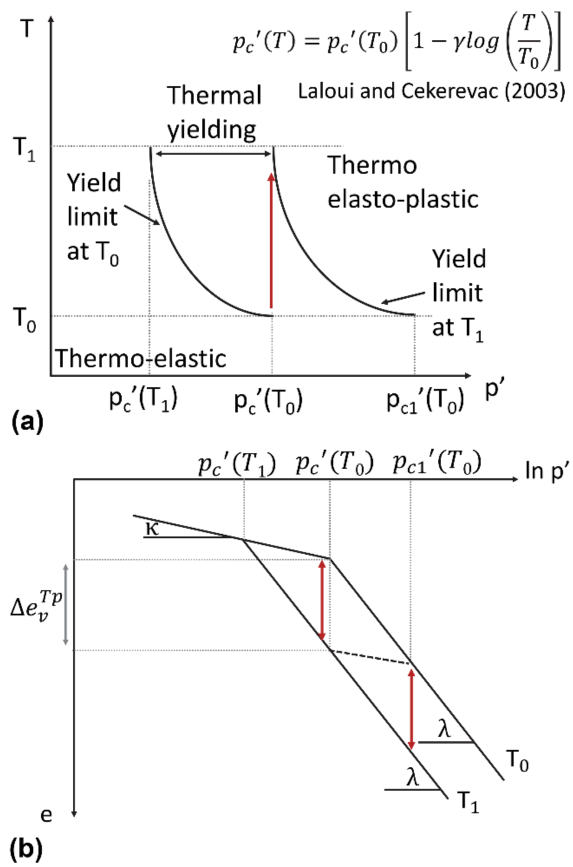

Fig. 2. Thermo-mechanical behavior of normally consolidated clays as predicted by the model of Laloui and Cekerevac (2003): (a) Thermal yield limit in T-p' plane; (b) Thermal volume change in e vs. ln p' plane

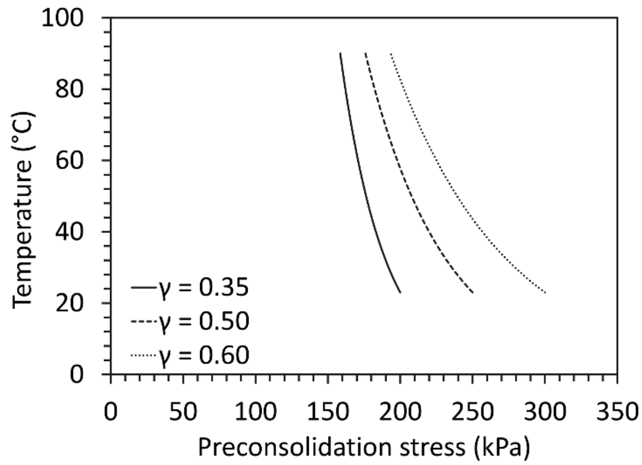

Fig. 3. Shapes of the yield curves showing variation in thermal preconsolidation stress with temperature at different initial mean effective stresses for normally consolidated clays

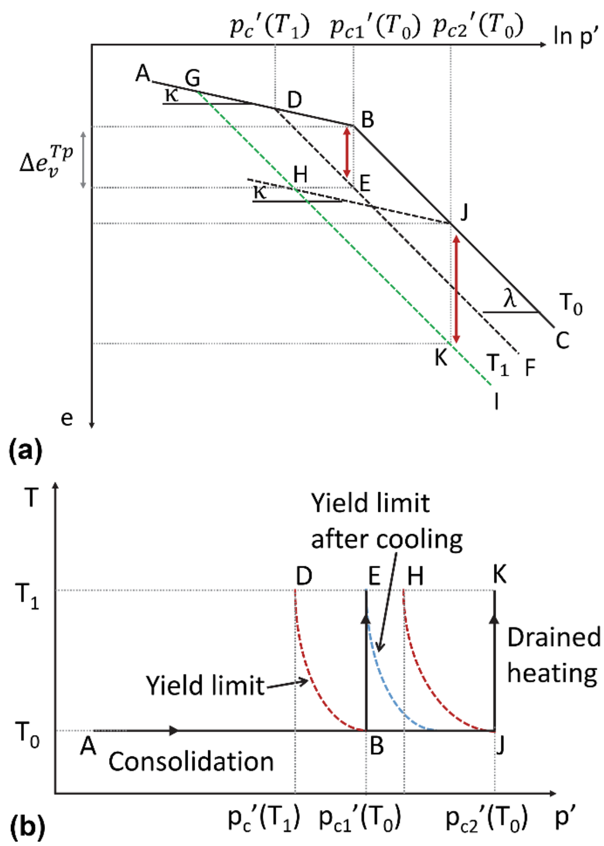

Fig. 4. New thermo-mechanical framework: (a) thermal volume change in e vs. ln p' plane; (b) thermo-mechanical paths in T-p' plane

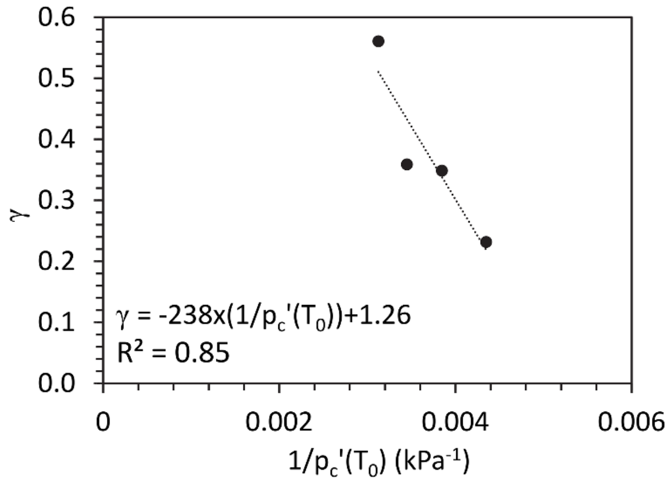

Fig. 5. Parameter γ as a function of mean preconsolidation stress for normally consolidated kaolinite (Data: Samarakoon et al. 2022)

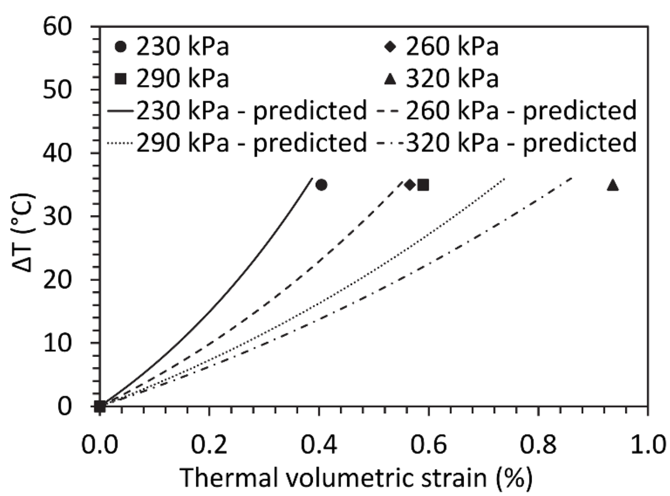

Fig. 6. Thermal volumetric strain of normally consolidated kaolinite at different initial mean effective stresses (Data: Samarakoon et al. 2022)

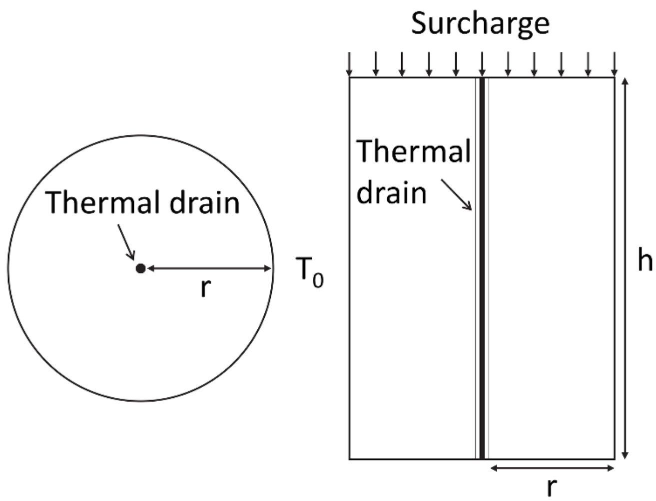

Fig. 7. Schematic diagram of the thermal drain arrangement in a finite soil domain

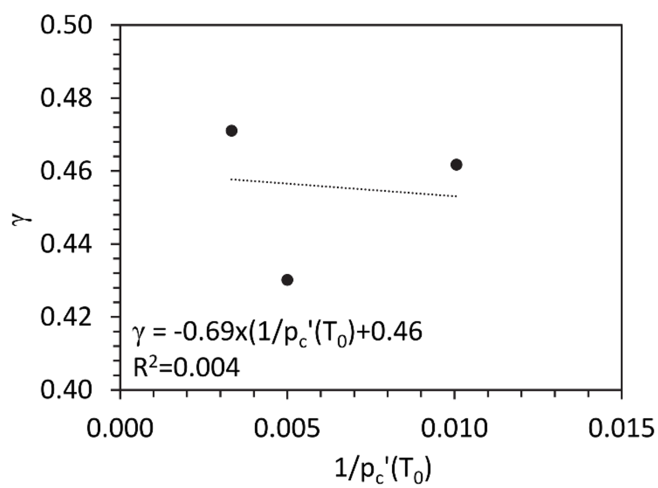

Fig. 8. Calibrated parameter γ as a function of mean preconsolidation stress for normally consolidated Bangkok clay (Data: Abuel-Naga et al. 2007)

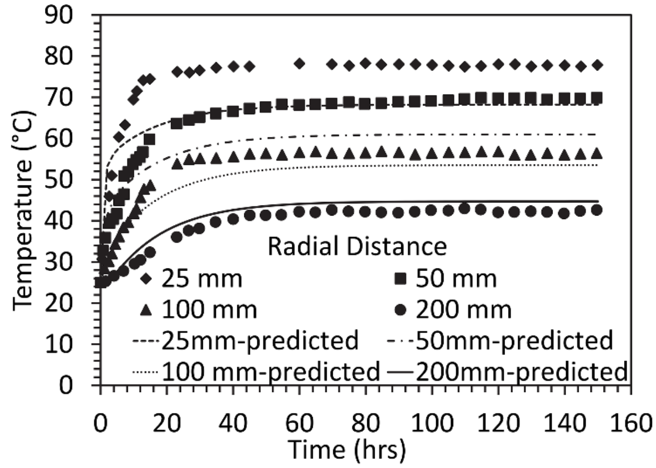

Fig. 9. Comparison of results for time series of temperature with data from Artidteang et al. (2011)

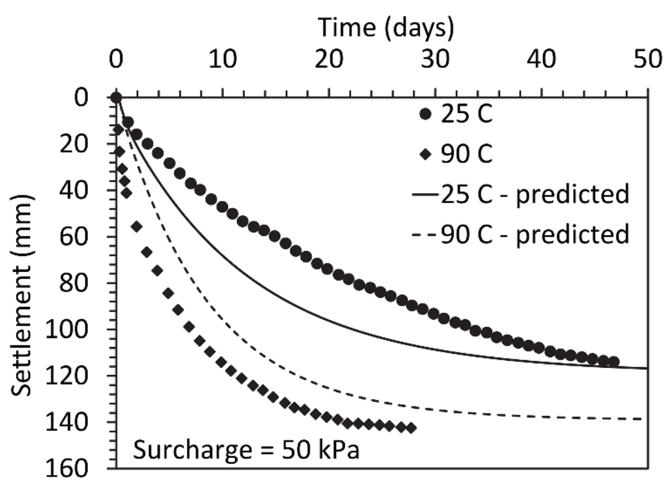

Fig. 10. Comparison of predicted results for settlement with data from Artidteang et al. (2011)

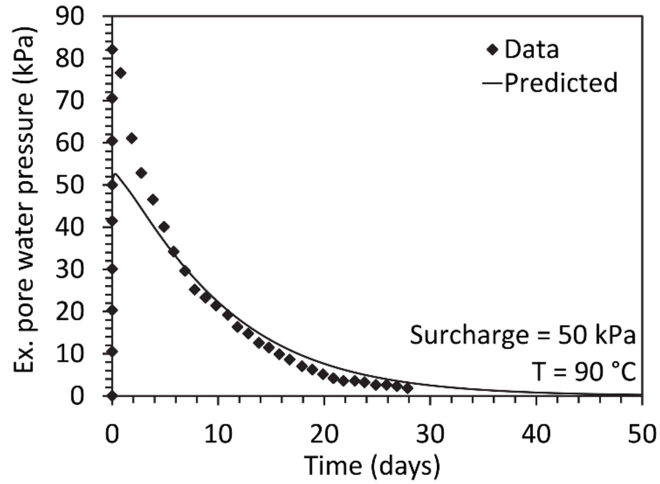

Fig. 11. Comparison of predicted results for excess pore water pressure generated with data from Artidteang et al. (2011)

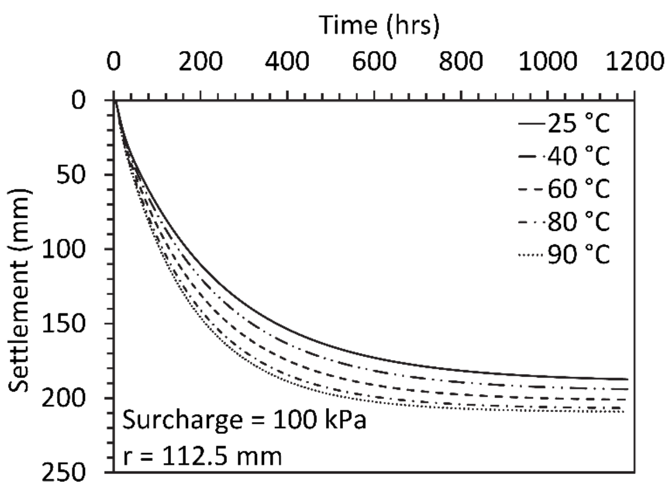

Fig. 12. Effect of temperature on consolidation settlement for a thermal drain combined with 100 kPa surcharge

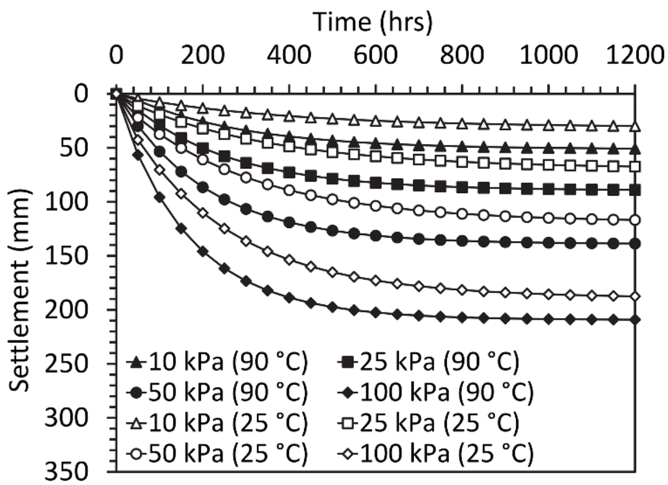

Fig. 13. Comparison of consolidation settlements at different applied surcharge stresses

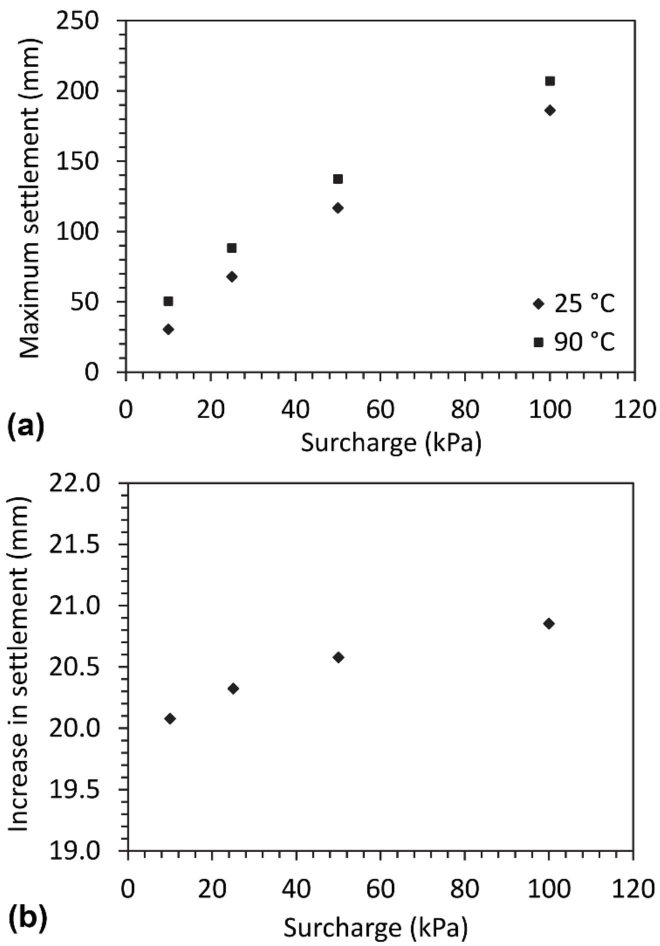

Fig. 14. (a) Effect of temperature and surcharge stress on the maximum settlement; (b) Increase in maximum settlement obtained when using a thermal drain at different surcharge levels

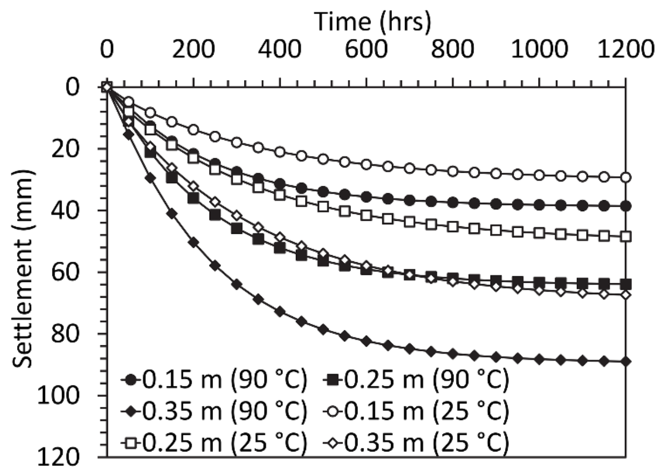

Fig. 15. Comparison of consolidation settlements obtained at different depths